Universitat Politècnica de Catalunya (UPC)
Universitat Autònoma de Barcelona (UAB)
Universitat de Barcelona (UB)
Institut de Ciències Fotòniques (ICFO)

http://www.photonicsbcn.eu

Master in Photonics

MASTER THESIS WORK

The nonlinear optics of first-order phase transitions

Alejandro del Bosque calvo

Cosupervised by Dr./Prof. Allan S. Johnson, (ICFO)
Cosupervised by Dr./Prof. Maciej Lewenstein, (ICFO)
Cosupervised by Dr./Prof Jose Francisco Trull, (UPC)

Presented on date 30th Augost 2022

Registered at

Escola Tècnica Superior d'Enginyeria de Telecomunicació de Barcelona

The nonlinear optics of first-order phase transitions

Alejandro del Bosque Calvo

Quantum Optics Theory/Ultrafast Dynamics Quantum Solids, ICFO – The Institute of Photonic Sciences, Castelldefels, Spain

E-mail: adelbosque42@gmail.com

30^{th} of August 2022

Abstract. Nonlinear effects are used to specially broaden the spectrum by the interaction with a material at high intensities. Here we study nonlinear effects in a light induced first-order phase transition of a thin layer of VO_2. The behaviour that we've found is a step-function evolution of nonlinear effects at the fluence threshold, where the phase transition happens. The spectrum broadens significantly from $\Delta\omega = 0.04$ rads/fs up to $\Delta\omega = 1.66$ rads/fs.

Keywords: Non-perturbative nonlinear optics, VO_2, first-order phase transition.

1. Introduction:

Nonlinear optics (NLO) has been studied since 1961 and now underpins many modern technologies. When a high intense source of light, usually a laser, hits a material it may change its optical response during its exposure. The interaction is referred to nonlinear because it does not depend linearly on the intensity of the electric field, but non-linearly.

NLO is characterized by the response of the material. Conventionally, the polarization in the material can be described as a power series expansion in the electric field strength $\tilde{E}$:

$$\begin{aligned}\tilde{P}(t) &= \epsilon_0 \left[\chi^{(1)}\tilde{E}(t) + \chi^{(2)}\tilde{E}^2(t) + \chi^{(3)}\tilde{E}^3(t) + \cdots\right] \\ &= \tilde{P}_L(t) + \tilde{P}_{NL}(t)\end{aligned} \tag{1}$$

where ϵ_0 is the permitivity in vacuum and χ are the susceptibilites of the material at different orders. $\chi^{(1)}$ correspond to the linear optics, $\tilde{P}_L(t) = \epsilon_0\chi^{(1)}\tilde{E}(t)$, while greater orders correspond to nonlinear optics, $\tilde{P}_{NL}(t)$.

The new frequencies are generated by the nonlinear polarization, which is stronger the more intense the light. In the perturbative limit, these effects scale with the powers

of the electric field. For instance, "second harmonic generation" (SHG), denoted by $\chi^{(2)}$, increases its strength as the square of light's intensity, and "third harmonic generation" (THG), which the denoted by $\chi^{(3)}$ grows as the cube of the light's intensity [1]. Beyond this simple picture are effects like "high harmonic generation" (HHG), for which the field strengths are so high that the perturbative approximation breaks down, and the signal shows an exponential increase with the field strength [2].

An alternative system for nonlinear optics is the light-induced phase transition. An ultrashort laser can induce a structural phase transition, where the optical properties of the new phase are different from the ground state. This change doesn't occur at a specific strength of the field but at a critical fluence, where the properties change sharply like a step-function switch [3]. Because this dependence on the fluence, a light-induced phase transition doesn't follow the field expansion model or even any function of field strength. Pump-probe measurements have been extensively used in the study of the dynamics of phase transitions [4, 5, 6, 7], but not from a nonlinear optics point of view. Critically, this transitions can be very fast, so that's why the changing of the optical properties are like a step-function in time when crossing over the threshold. This behaviour is called "threshold-switching" and this effects on the driving pulse have been seen with picosecond electrical pulses [8] but not yet with femtosecond light pulses.

Here, we will study the optical properties of the "threshold-switching" phenomena of VO_2 from a nonlinear optics perspective. To do so, we will construct a model to study the reflected light during the phase transition at different fluences and pulse durations.

2. Model

VO_2 has three phases in its solid state: a rutile metallic phase (R) and two insulating monoclinic phases (M_1 and M_2) [9]. When a femtosecond pulse laser hits on the crystal, a photoinduced phase transition may occur from the insulator phase M_1 to the metallic phase R. This transition occurs when the energy induced by the laser gets larger than the so called threshold energy. Sometime later after the pulse stops striking, the crystal relaxes to its previous phase.

When the phase changes, it changes the sample reflectivity. Because the change is extremely fast, the order of a few femtoseconds [10], it takes place while the pulse is propagating through the material. In other words, the temporal shape of the pulse is modified during the phase transition as the reflectivity changes, so it will cause a broadening of the spectrum.

However, in real crystals this change is not infinitely sharp but is broadened by the initial range of domains of crystallities leading to a range of transition temperatures. Figure 1 represents the transmission of VO_2 at different temperatures. The change of

transmission is due to the phase transition of the material. We see that, for a real crystal, the transmission doesn't change instantaneously at a critical certain critical temperature, smoothly along a temperature range [11]. To understand how this practically impacts the effect and how much spectral broadening can we expect from a real system, we will model the behaviour of the reflected light as a function of the fluence and the pulse duration.

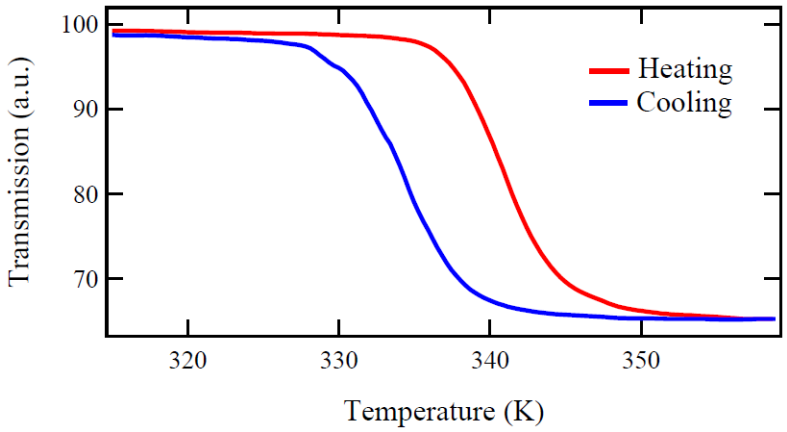

Figure 1: Temperature-dependent optical transmission of a polycrystaline VO_2 as it passes through the phase transition, reproduced from reference [11]. The transition is broadened because of nanoscale inhomogeneity.

We will use the data from figure 1 to obtain the distribution of the different critical temperatures.

$$D = \frac{\partial Transmission}{\partial T_c} \tag{2}$$

It is not clear if the phase transition by photoinduction is caused by thermal effects, because thermal effects are slow in time. However, it has been shown that the critical fluence, the optical energy per unit area needed to trigger the transition, closely follows the thermal energy required [12]. The thermal energy is the necessary energy to bring from a initial temperature up to the one where the phase transition occurs. We can relate this energy to the fluence in order to relate the critical thermal distribution of equation 2 to a critical fluence distribution.

To do so, we integrate the heat capacity of VO_2 [13], shown in figure 2, over the temperature, from room temperature to a critical temperature, to obtain the energy required to induced the phase transition. We will do this integration for different critical temperatures to obtain its correspondent value of thermal energy:

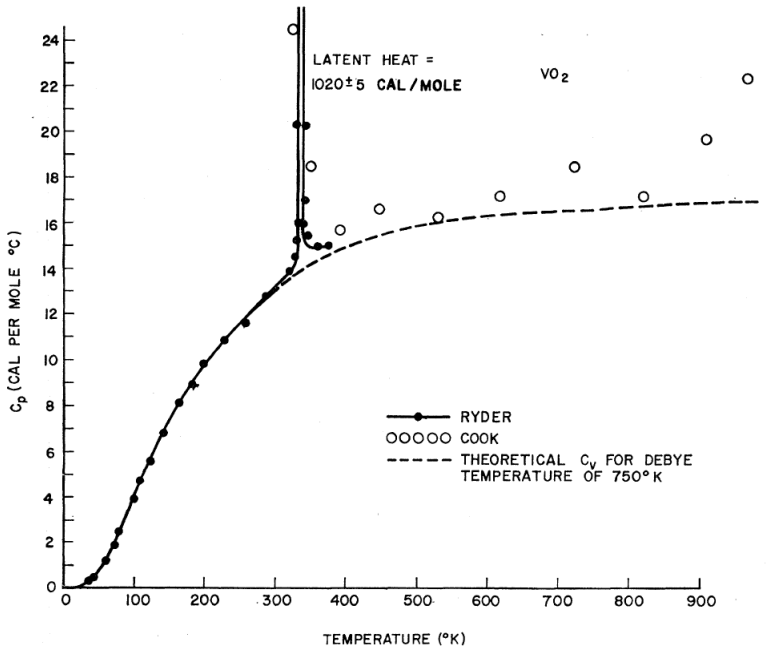

Figure 2: Data of heat capacity of VO_2 represented from reference [13].

$$E_T = \int_{T_i}^{T_c} c_v dT \tag{3}$$

where T_i and T_c are the initial and critical temperature, c_v heat capacity and E_T is the thermal energy. We treat the variation in T_c for the different crystallites as an effective shift in T_i, which is equivalent to first order in a shift in overall c_v curve. Then knowing the value for the thermal energy at different temperatures we obtain the critical fluences [14] from each value of E_T:

$$F_c = \frac{dE_T}{1-R} \tag{4}$$

where d is the penetration depth, with a value of 62 nm, and R is the reflectivity of the sample, 0.18 [14]. Since each critical fluence is assigned to a critical temperature, so we can obtain a distribution of critical fluences from equation 2.

Now, with the fluences obtained from equation 4, we seek the instant of time during the pulse when it will undergo the phase transition, assigning to each critical time a weighting according to the distribution value from equation 2, $D(T_c) = D(F_c)$ from which we reconstruct the overall material response. To know at which time this will occur, we set a Dirac delta function that will have value 1 at that time when the fluence applied is equal to the critical one. This will tell us at which time the transition will occur. But, since the phase transition in a real material is, while very fast in time, finite, we will use an erf function of 5 femtoseconds width instead to simulate that fast transition. This leads us to an overall expression for the signal as:

$$Signal(t) = \frac{1}{2}\int D(F_c)\cdot erf\left(\frac{t\cdot(1-\delta(F-F_c))+5}{5}+1\right)dF_c \tag{5}$$

With the data obtained from equation 5, we can see when VO_2 will start to change phase and how quickly in time for each fluence that we apply. Since the signal overlaps in time with the pulse, the phase transition will have a back-reaction on the driving pulse. This will tell us which fraction of the pulse will be reflected by the M_1 or R-phase. So, knowing that the reflectivity for the M_1 phase is 0.15 and for R-phase is 0.3 (both measured at normal incidence with a white light lamp in our lab) we will see the shape in time of the reflected pulse for different fluences, as shown in figure 3.

.

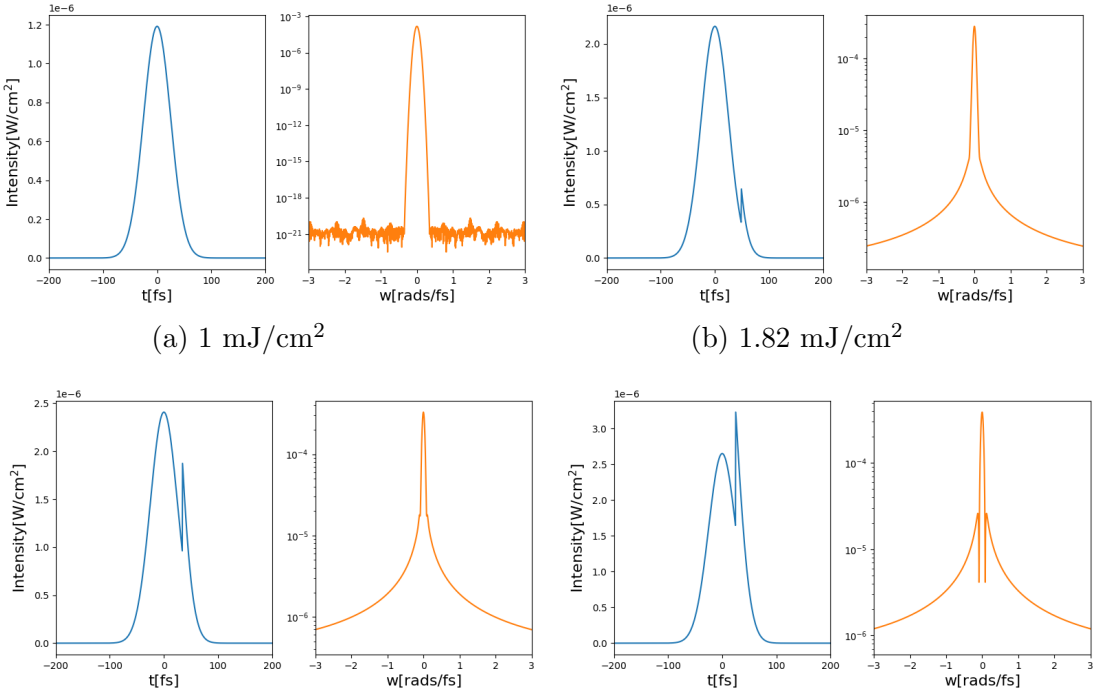

(a) 1 mJ/cm^2 (b) 1.82 mJ/cm^2

(c) 2 mJ/cm^2 (d) 2.22 mJ/cm^2

Figure 3: A 35 fs pulse reflected on a VO_2 thin layer at different fluences. The plot on the left represents the time domain while the right one represents its spectrum. In 3b the theshold fluence is reached, 1.82 mJ/cm^2,and the sample begins to transform, changing it's reflectivity. Due to this, the spectrum suddenly shows a large broadening.

As we see in figure 3, the pulse is constant while increasing the fluence until we reach critical fluence at 1.82 mJ/cm^2, where the reflectivity starts to change and shifts the shape of the temporal pulse abruptly. Because of this, the spectrum, represented

on the right, suddenly broadens with this minimum change.

In figure 4 we represented the evolution of the spectrum width for a fixed fluence and then for a fixed pulse duration:

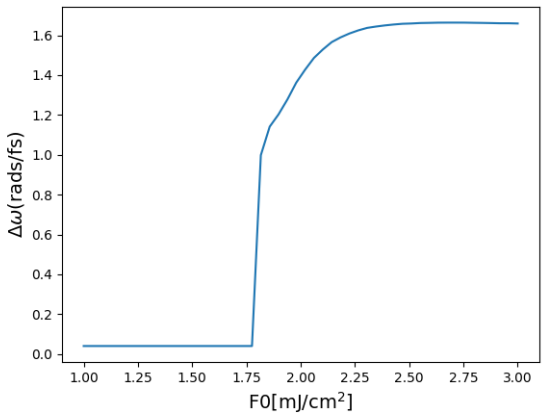

(a) Evolution for t_0=35.50 fs

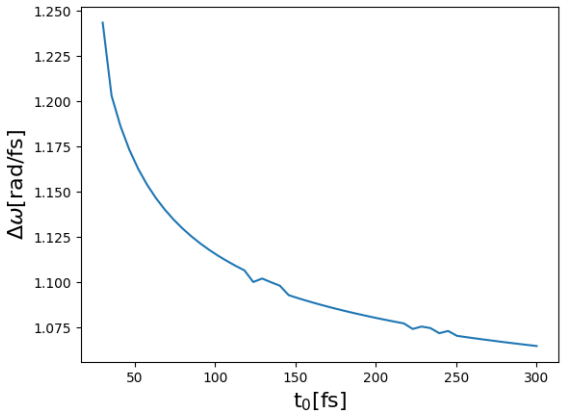

(b) Evolution for F_0=1.90 mJ/cm^2

Figure 4: Evolution of the spectral width for (a) constant pulse duration and (b) constant fluence over the threshold.

In figure 4a we see that at the threshold fluence has a sudden big jump from 0.04 rads/fs up to 1.66 rads/fs, almost 100 times wider. This threshold switch effect has a strong dependence on the fluence and a weak one on the time pulse duration, so we can get a abrupt evolution of the spectrum width at this critical fluence. Also we see that the blurring from a realistic polycristall ine sample doesn't strongly effect it, as the effect is clearly visible and dramatic.

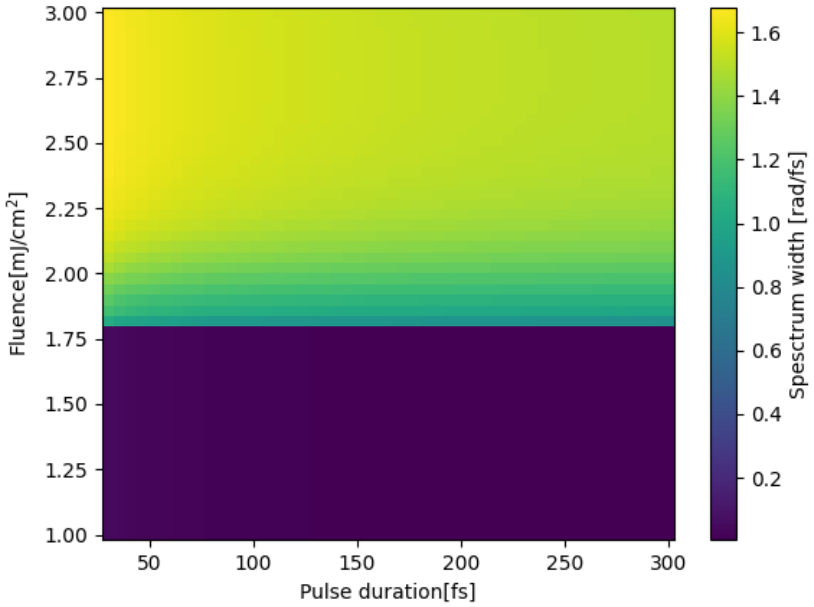

Figure 5: Spectrum widths for different pulse durations and fluences. The spectrum is constant as a function of fluence below the criticla fluence, where the bandwidth increases roughly

On figure 5 we represented the standard deviation of pulse's spectrum to see how much it change its width with the pulse duration and the fluence. For a constant pulse duration, the spectrum below threshold has a value constant (for t_0=35.50 fs is 0.04 rads/fs), but above threshold has a big jump and starts to grow until F_0=3 mJ/cm^2. For a constant fluence the spectrum doesn't change too much, but it shrinks the longer the pulse is.

Since there is no much change for the pulse duration axis, we will prepare an experimental setup to study the transmitted laser pulse at 800 nm and a pulse duration of $t_0 = 30fs$.

3. Experimental

The sample of VO_2 is a thin layer of 60 nm thick that has been grown on a sapphire substrate approximately 1 mm thick. We have measured the fluence threshold in this sample with ultrafast pump-probe to be 6 mJ/cm^2. We will measure the transmitted light through the sample at normal incidence. To do so, we've prepared a spatial phase interferometry (SPI) [15] and Grenouille [16] setup, see figure 6.

We split the pulse in two parts with a beam splitter; one as the signal, which will pump the sample, and the other as a reference pulse. Both will have the same optical

path length at the beginning. The signal will pass through the VO_2 and then through a set of mirrors on a moving table, which will used to apply a time delay. The reference pulse will be reflected on a flipped mirror, where it can direct the pulse to the Grenouille to characterize the pulse. Then, we set a delay in the signal pulse and both pulses will be recombined at the interferometer. We will study changes in the signal pulses at different fluences set by the fluence controller, which is composed with a waveplate and a polarizer.

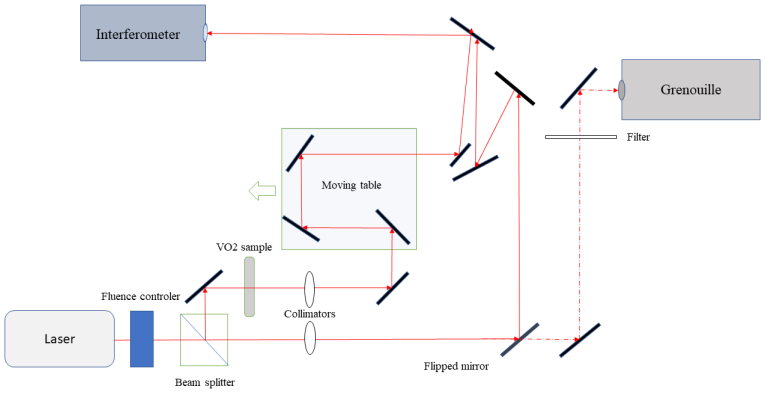

Figure 6: Spectral phase interferometry setup for characterize the phase transmision induced change in the pump.

In figure 7 we present the data from the Grenouille, which gives us information about the phase of the reference pulse.

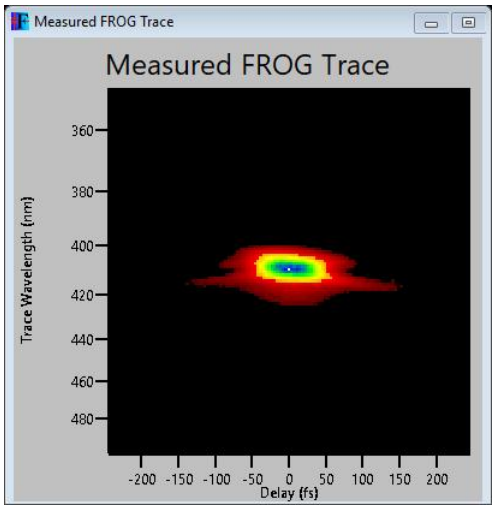

(a) FROG trace of the reference pulse.

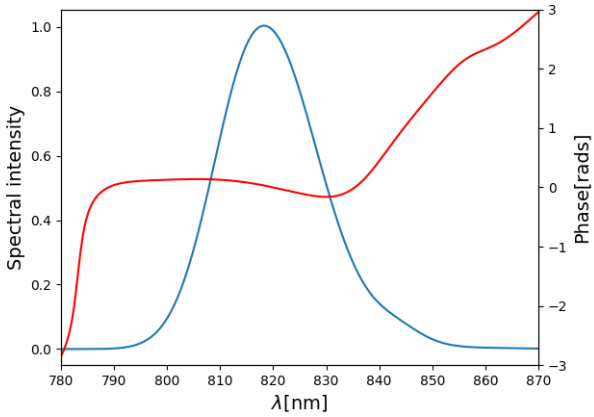

(b) Spectral phase and intensity of the reference pulse.

Figure 7: Reference pulse characterization obtained from the Grebouille.

The SPI signal in the spectrometer is given by:

$$S_{FTSI}(\omega) = S_{signal} + S_{ref} + 2\sqrt{S_{signal}(\omega) + S_{ref}(\omega)}\cos(\Psi_{signal} - \Psi_{ref} + \omega\tau)) \qquad (6)$$

where S_{ref} and S_{signal} are the intensities for the reference and signal pulse, measured blocking one arm and then the other on the interferometer, Ψ_{ref} and Ψ_{signal} are their respective phases and ω and τ are the frequency at we measured in the spectrometer and time delay of the pulse [17]. The measured spectrum is represented in figure 8 at different fluences, adjusting the exposure to ensure optical S/N for each fluence.

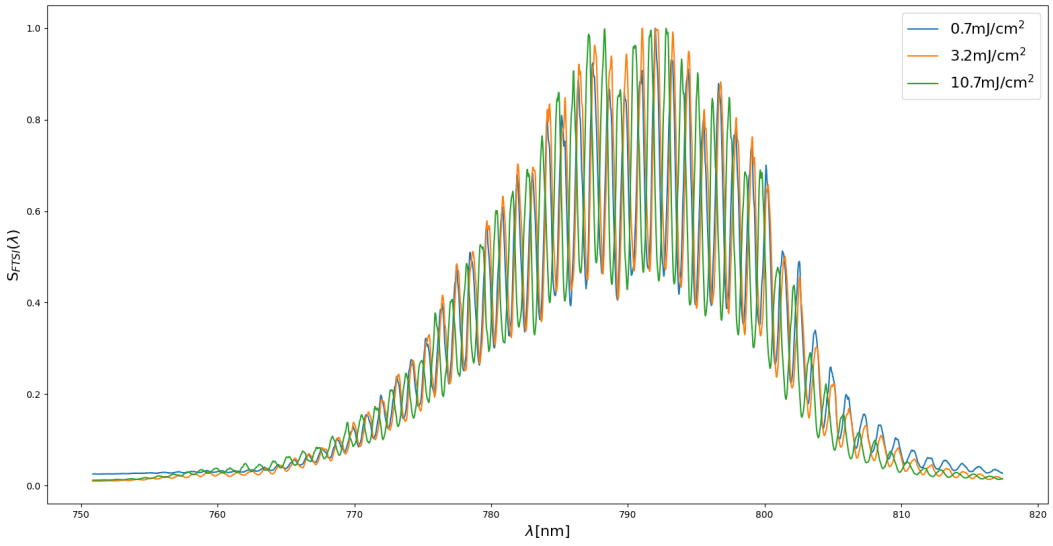

Figure 8: Normalized interference of the reference pulse and the signal one at different fluences.

We can see in figure 8 that the fringes are in phase for both fluences below the phase transition, 6 mJ/cm^2 in this sample, but show a dramatic shift above it. The fringes map the phase different between Ψ_{signal} and Ψ_{ref}, so this displacement means that the phase of the pulse changes over the threshold fluence. This is because the phase transition of VO_2 changes the shape of the temporal pulse, modifying its transmitivity. Further analysis is necessary to reconstruct the time-domain structure of the signal pulse in the two limits.

4. Conclusions

Firs-order phase transitions offer a new type of nonlinear optics, presenting a huge change in optical properties once the threshold fluence is reached. In our model we predict a huge broadening and a minimal effect of polycrystalinity, suggesting the effect should be experimentally observable. Then, we measured this effect in the lab using SPI and see that the phases changes with the fluence, presenting there the effect on the spectrum by the phase transition. The phases change with the fluence because the phase transition is affecting the incident light.

5. References:

[1] Boyd R W 2020 *Nonlinear optics* (Academic press)

[2] Popmintchev T, Chen M C, Popmintchev D, Arpin P, Brown S, Ališauskas S, Andriukaitis G, Balčiunas T, Mücke O D, Pugzlys A *et al.* 2012 *science* **336** 1287–1291

[3] Lopez R, Haglund Jr R F, Feldman L C, Boatner L A and Haynes T E 2004 *Applied physics letters* **85** 5191–5193

[4] Fedotov V, MacDonald K and Zheludev N 2005 *Journal of Optics A: Pure and Applied Optics* **7** S241

[5] Gallmann L, Sutter D, Matuschek N, Steinmeyer G, Keller U, Iaconis C and Walmsley I 1999 *Optics letters* **24** 1314–1316

[6] Lisewski J, Heathcote J, Petrov G I and Yakovlev V V 2005 Optical pulse-shaping using ultrafast phase transformation in vanadium dioxide *Ultrafast Phenomena in Semiconductors and Nanostructure Materials IX* vol 5725 (SPIE) pp 91–97

[7] Zheludev N 2002 *Contemporary Physics* **43** 365–377

[8] Zalden P, Shu M J, Chen F, Wu X, Zhu Y, Wen H, Johnston S, Shen Z X, Landreman P, Brongersma M *et al.* 2016 *Physical Review Letters* **117** 067601

[9] Park J H, Coy J M, Kasirga T S, Huang C, Fei Z, Hunter S and Cobden D H 2013 *Nature* **500** 431–434

[10] Jager M F, Ott C, Kraus P M, Kaplan C J, Pouse W, Marvel R E, Haglund R F, Neumark D M and Leone S R 2017 *Proceedings of the National Academy of Sciences* **114** 9558–9563

[11] Vidas L, Gunther C M, Miller T A, Pfau B, Perez-Salinas D, Martínez E, Schneider M, Guhrs E, Gargiani P, Valvidares M *et al.* 2018 *Nano Letters* **18** 3449–3453

[12] Kübler C, Ehrke H, Huber R, Lopez R, Halabica A, Haglund Jr R and Leitenstorfer A 2007 *Physical Review Letters* **99** 116401

[13] Berglund C and Guggenheim H 1969 *Physical Review* **185** 1022

[14] Vidas L, Schick D, Martínez E, Perez-Salinas D, Ramos-Álvarez A, Cichy S, Batlle-Porro S, Johnson A S, Hallman K A, Haglund Jr R F *et al.* 2020 *Physical Review X* **10** 031047

[15] Iaconis C and Walmsley I A 1999 *IEEE Journal of quantum electronics* **35** 501–509

[16] Akturk S, Kimmel M, O'Shea P and Trebino R 2003 *Optics Express* **11** 491–501

[17] Fernández B A 2012 *Spatiotemporal characterization of ultrashort laser pulses* Ph.D. thesis Universidad de Salamanca